

# Poroelastic longitudinal wave equation for soft living tissues

Piero Chiarelli\*<sup>1,2</sup>, Bruna Vinci<sup>1</sup>, Antonio Lanatà<sup>2</sup>, Clara Lagomarsini<sup>2</sup>, Simone Chiarelli<sup>3</sup>

*(1) National Council of Research of Italy, Moruzzi, 1 - 56100 Pisa – Italy  
and*

*(2) Interdepartmental Research Center “E. Piaggio”, Faculty of Engineering, University of Pisa, via Diotisalvi, 2  
-56126 Pisa, Italy*

*(3) School of Engineering, University of Milan, via Bramante, 65 I-26013 Crema (CR,) Italy*

## Abstract

Making use of the poroelastic theory for hydrated polymeric matrices, the ultrasound (US) propagation in a gel medium filled by spherical cells is studied. The model describes the connection between the poroelastic structure of living means and the propagation behavior of the acoustic waves. The equation of fast compressional wave, its phase velocity and its attenuation as a function of the elasticity, porosity and concentration of the cells into the gel external matrix are investigated. The outcomes of the theory agree with the measurements done on Alginic acid gel scaffolds in-seminated by porcine liver cells at various concentrations. The model is promising in the quantitative non-invasive estimation of parameters that could assess the change in the tissue structure, composition and architecture.

**Running title:** US poroelastic tissue assessment

**Keywords:** Ultrasound, non-invasive assessment of biological tissue, poroelastic model of living tissues, high frequency poroelastic waves in soft tissues

## 1. Introduction

The description of US waves in soft biological hydrogels of natural tissue is still lacking. Nowadays, the US propagation in natural hydrogels, mostly composed of water, is usually modeled by

means of the wave equation that holds for liquids [1] and the effect of the chemical water-polymer interaction on the US propagation in natural hydrogels and tissue is described by modeling them as water-polymer solutions [2].

On the other hand, the poroelastic theories are able to describe the features of the US propagation depending from the liquid-solid arrangement.

For instance, the liquid-like model is not able to explain the relevant sound speed difference between gels and its pure interstitial fluid even if it has a concentration as high as 98%.

Even if the chemical and the rheological aspects are very important for the propagation of elastic waves, the liquid-like approach and the poroelastic one are completely disconnected.

The integration of the two models has been hindered by the fact that the poroelastic model are not satisfying in the description of US propagation in hydrogels showing important discrepancies with experiments.

Actually, tissues may have bounded resonant states [2] with the US attenuation showing a frequency ( $\nu$ ) law [3]:  $\nu^{(1+\delta)}$ , with  $\delta$  ranging between  $\frac{1}{4}$  and  $\frac{1}{2}$  ( $\delta = 1$  for water).

At high frequencies the classical poroelastic theories, mainly developed for geological studies, [4-11] are unable to explain the fractional value of  $\delta$  for the frequency dependence of the US attenuation.

Recently the authors [12] have proposed and validated a poroelastic model for US in hydrogels [12] having a frequency dependence of attenuation with fractional values of  $\delta$ .

This result is obtained by introducing the bounded water interaction between the polymer network and the free water.

The poroelastic model for gels, obtained by introducing the “chemical interaction” of the bounded water between the polymer network and the interstitial fluid opens the way to obtain integrated poroelastic-chemical model for gels and possibly for biological tissue, even if they are far to be homogenous but present anisotropies such as blood vessels and cells.

In the present work spherical cells are considered into the environment of a hydrogel matrix. The biological cells are designed as poro-elastic spheres, endowed by internal and superficial elasticity as well as permeability, and are assumed to be isotropically dispersed in the extra-cellular hydrogel. The model is developed in the continuum limit approach for US wavelength much bigger than the cells dimension (typically up to about 10 MHz).

This paper analyzes also the development of a non-invasive tissues assessment technique by monitoring the permeability of the cells and the ECM. The detection of the liver cirrhosis can be one of the short term application of this work [13]. About the long term objectives of this study there are the development of non-invasive US methods [14-18].

The renal denervation and the functional modulation of biological functions in tissues and organs can also benefit from the present research.

## **2. Poro-elastic US wave in soft living tissues**

### *2.1. US wave in highly hydrated gels*

The poroelastic wave equations for hydrogels is obtained by introducing the appropriate fluid network interaction that takes into account for the bounded water presence around the polymer chains [2 12]. Under the assumption that the bounded water volume fraction is very small and that the “polymer-bounded water aggregate” constitutes the solid matrix of the poroelastic mean, it is possible to end with the following motion equations [12]

$$\nabla^2 (Re_{\alpha\alpha}) = \beta_e^2 \partial^2 (\beta_e \rho_f e_{\alpha\alpha}) / \partial t^2 + \beta_e \partial^2 \rho_{11} (\varepsilon_{\alpha\alpha} - e_{\alpha\alpha}) / \partial t^2 \quad (1.a)$$

$$f \partial (e^*_{\alpha\alpha} - e_{\alpha\alpha}) / \partial t \cong (Q/R) \partial^2 (\beta_e \rho_f e_{\alpha\alpha}) / \partial t^2 \quad (1.b)$$

$$\beta_e f \partial (e^*_{\alpha\alpha} - e_{\alpha\alpha}) / \partial t = \eta(\omega) \partial (\varepsilon_{\alpha\alpha} - e^*_{\alpha\alpha}) / \partial t + K (\varepsilon_{\alpha\alpha} - e^*_{\alpha\alpha}) \quad (1.c)$$

$$\beta_e = \beta - \phi \quad (2)$$

where  $\varepsilon_{ij}$  is the solid strain tensor,  $e_{\alpha\alpha}$  is the trace of the liquid strain tensor,  $e^*_{\alpha\alpha}$  is the trace of the bounded water strain tensor;  $Q$ , and  $R$  are the poroelastic constants of the medium that can be measured by means of jacketed and unjacketed experiments [19];  $\beta$  is the water volume fraction of the hydrogel,  $\phi$  is the volume fraction of bounded water,  $\beta_e$  is the effective free water volume fraction,  $f$  is the inverse of the hydraulic permeability of the matrix [19], and  $\rho_{11}$ ,  $\rho_{12}$  and  $\rho_{22}$ , are the mass densities parameters defined as:  $\rho_{11} + 2\rho_{12} + \rho_{22} = \rho$ ,  $\rho_{11} + \rho_{12} = (1 - \beta_e)\rho_s$ ,  $\rho_{12} + \rho_{22} = \beta_e \rho_f$ ; where  $\rho_s$  and  $\rho_f$  represent the solid and the liquid mass densities respectively, while  $\rho$  is the total mass density of the medium. Moreover,  $K$  and  $\eta$  are the elastic constant and the friction coefficient describing the polymer-bounded water interaction, respectively.

The above equations are derived with the assumption that [12] the inertial effect of bounded water can be disregarded and that the trace of the strain tensor of the polymer  $\varepsilon_{\alpha\alpha}$  approximates that one of the solid aggregate.

Under this assumptions, considering the fast plane wave  $e_{\alpha\alpha} \propto e^{-\alpha x} e^{i(kx - \omega t)}$  equation (1.c) reads

$$\beta_e f \partial (e^*_{\alpha\alpha} - e_{\alpha\alpha}) / \partial t = F(\omega) \partial (\varepsilon_{\alpha\alpha} - e_{\alpha\alpha}) / \partial t \quad (3)$$

where the complex friction coefficient  $F(\omega)$  of the gel reads

$$F(\omega) = [(\beta_e f)^{-1} + (\eta(\omega) + (K(\omega) / \omega))^{-1}]^{-1} \quad (4)$$

leading through (1.a) to the characteristic equation

$$(k + i\alpha)^2 = \omega^2 \rho_f (\beta_e^3 / R) (1 - i\omega(1 - \beta_e) \rho_{11} / F(\omega)) \quad (5)$$

that split in the real and imaginary part leads to

$$c^2 = c_0^2 (1 + \alpha^2 / k^2) / (1 + \beta_e^{-2} (1 - \beta_e) \omega \rho_{11} \text{Im}\{F(\omega)^{-1}\}) \quad (6)$$

$$2\alpha / k = -(c / c_0)^2 \omega (1 - \beta_e) \rho_{11} \text{Re}\{F(\omega)^{-1}\} \quad (7)$$

where

$$c_0 \cong c_f / (\beta - \phi)^{3/2} \quad (8)$$

is the pure elastic longitudinal US wave velocity,  $c_f = (R/\rho_f)^{1/2}$  its velocity in the intermolecular fluid (free water) and

$$\text{Re}\{F^{-1}\} = [\eta(1 + \eta / \beta_e f) + (K^2 / \beta_e f \omega^2)] / (\eta^2 + (K / \omega)^2) \quad (9)$$

$$\text{Im}\{F^{-1}\} = -(K / \omega) / (\eta^2 + (K / \omega)^2). \quad (10)$$

By solving equation (6,7) in  $\alpha$  (i.e., the US attenuation coefficient) we obtain

$$(2\alpha / k) / (1 + \alpha^2 / k^2) = -\omega(1 - \beta_e) \rho_{11} \text{Re}\{F(\omega)^{-1}\} / (1 + \beta_e^{-2} (1 - \beta_e) \omega \rho_{11} \text{Im}\{F(\omega)^{-1}\}) \quad (11)$$

that for  $(\alpha / k)^2$  very small (of order of  $10^{-3}$  in hydrogels) reads

$$(2\alpha / k) \cong -\omega(1 - \beta_e) \rho_{11} \text{Re}\{F(\omega)^{-1}\} / (1 + \beta_e^{-2} (1 - \beta_e) \omega \rho_{11} \text{Im}\{F(\omega)^{-1}\}). \quad (12)$$

Assuming that the polymer-bounded water viscosity  $\eta(\omega)$  follows the frequency behavior [12]

$$\eta(\omega) = \eta_0 (\omega_g / \omega)^\delta \quad (13)$$

where  $0 < \delta \leq 1/2$  and where  $\omega_g = 2\pi \eta_0 / \rho_f$ , it follows that

$$\lim_{\omega/\omega_g \gg 1} \text{Re}\{F^{-1}\} \cong 1/\eta(\omega) \quad (14)$$

$$\lim_{\omega/\omega_g \gg 1} \text{Im}\{F^{-1}\} \cong 0 \quad (15)$$

Thence, equations (6-7) in the high frequency limit read

$$c^2 = c_0^2 (1 + \alpha^2 / k^2) \cong c_0^2 \quad (16)$$

and

$$2\alpha / k = -(c / c_0)^2 (\omega / \omega_g)^{1+\delta} (1 - \beta_e) \sigma_{pf} \quad (17)$$

where

$$\sigma_{pf} = 2\pi \rho_{11} / \rho_f. \quad (18)$$

Finally, when the polymer network is not very diluted, but has an appreciable polymer concentration, the series expansion as a function of the fraction of polymer volume  $(1 - \beta)$  can be introduced into equation (8) as follows [12]

$$c_0^2 \cong c_f^2 / [(\beta - \phi)^3 + \chi_1(1 - \beta) + \chi_2(1 - \beta)^2] \quad (19)$$

## 2.2. US wave equation in a hydrogel with dispersed cells

When we describe a tissue as a hydrogel poroelastic mean containing cells, we have to refer to the overall tissue constants  $\beta_t, R_t, \rho_f, F_t$  and so on. By introducing (1.b) into (1.a) at lowest order for the tissue we obtain

$$\nabla^2 (R_t e_{\alpha\alpha}) \cong \beta_{et}^2 \partial^2 (\beta_{et} \rho_f e_{\alpha\alpha}) / \partial t^2 + \beta_{et} (1 - \beta_{et}) F_t^{-1} \partial^3 \rho_{11} e_{\alpha\alpha} / \partial t^3 \quad (20)$$

where

$$\nabla^2 (R_t e_{\alpha\alpha} / \rho_f) \cong \beta_{et}^3 \partial^2 e_{\alpha\alpha} / \partial t^2 \quad (21)$$

represents the zero order elastic wave equation. Moreover, we name the total water volume fraction, the bounded water volume fraction and the free water volume fraction for the cells, for the ECM and for the tissue by adding the suffixes c, g and t, respectively, as in the following

$$\beta_{eg} = \beta_g - \phi_g \quad (22)$$

$$\beta_{ec} = \beta_c - \phi_c \quad (23)$$

$$\beta_{et} = \beta_t - \phi_t \quad (24)$$

By defining  $\gamma$  as the fractional volume of cells inside the tissue as

$\gamma = \text{total volume of cells} / \text{total volume of tissue}$ ,

the mean fractional water content of the tissue  $\beta_t$  reads

$$\beta_t = (1 - \gamma) \beta_g + \gamma \beta_c = \beta_g \{1 - \gamma (1 - \beta_c / \beta_g)\} \quad (25)$$

### 2.3. US speed in natural tissue

In order to investigate the US phase velocity in the hydrogel-cells syncytium we need to determine the poroelastic parameters concerning the inertial and elastic terms in the motion equations.

As far as it concerns the compressibility modulus  $R_t$  and the mass density of the fluid (free water)  $\rho_f$  of the syncytium they are influenced by the chemical (e.g., ionic strength) and mass composition of the cells that, generally speaking, may differ from that ones of the ECM. As a consequence of this, in principle,  $c_{t0} = (R_t/\rho_f)^{1/2}$  and the elastic phase velocity  $c_{0t}$  are function of cell concentration  $\gamma$ .

Assuming that the variation of the ratio  $R_t/\rho_f$  is small compared to that one of the external matrix  $R/\rho_f$ , the series expansion

$$c_{tf} = (R_t/\rho_f)^{1/2} \cong c_f^2 \{1 + A_1\gamma + A_2\gamma^2\} \quad (26)$$

can be assumed for the tissue.

Moreover, since for a biological tissue  $\alpha_t/k \ll 1$ , analogously to equations (16,19) we write

$$c_t = c_{t0}(1 + (\alpha_t/k)^2)^{1/2} \cong c_{t0} \quad (27)$$

and hence given that

$$c_{t0}^2 \cong c_{tf}^2 / [(\beta_t - \phi)^3 + \chi_1(1 - \beta_t) + \chi_2(1 - \beta_t)^2] \quad (28)$$

we obtain

$$c_t^2 \cong c_f^2 \{1 + A_1\gamma + A_2\gamma^2\} / [(\beta_t - \phi)^3 + \chi_1(1 - \beta_t) + \chi_2(1 - \beta_t)^2] \cong c_g^2 \{1 + A_1\gamma + A_2\gamma^2\} \quad (29)$$

where  $c_g$  is given by the identities (16, 19).

#### 2.4. US attenuation in natural tissue



In this section we derive the complex friction coefficient (the inverse of hydraulic conductance of the syncytium) that is responsible for the US attenuation.

We assume in the following the complex hydraulic conductance:

- i.  $F_{g(\omega)}^{-1} \cong \eta_g^{-1}$  for the extra-cellular hydrogel
- ii.  $F_{c(\omega)}^{-1} \cong \eta_c^{-1}$  for the internal jelly cell body
- iii.  $F_{m(\omega)}^{-1}$  for the cells membrane.

For sinusoidal inputs of frequency  $\omega/2\pi$  we also assume that

$$F_{m(\omega)}^{-1} = K_m + i\omega b E_m^{-1} \quad (30)$$

where the real part  $K_m$  is the hydraulic permeability of the cell membrane and the imaginary one is its superficial compliance proportional to the inverse of Young's elastic modulus  $E_m$ . In the case where the cell membrane thickness is much smaller than the cell diameter  $a$ ,  $b^{-1}$  coincides with the membrane thickness.

For sinusoidal pressure inputs the overall conductance of the tissue[20] reads

$$F_t^{-1} = F_g^{-1} [2(1-\gamma)F_g^{-1} + (1+2\gamma)F_c^{-1}] / [(2+\gamma)F_g^{-1} + (1-\gamma)F_{cm}^{-1}] \quad (31)$$

Where  $F_{cm}^{-1}$  is a combined membrane permeability that reads

$$F_{cm}^{-1} = F_c^{-1} a F_m^{-1} / (F_c^{-1} + a F_m^{-1}) \quad (32)$$

In order to apply the above model to a biological tissue we need to single out the relative magnitude of the hydraulic constants. Since the superficial membrane of the cells has a very low hydraulic

permeability (it separates the inner cell body from the external hydrogel matrix), we expect that the frequency  $\omega_m / 2\pi = K_m b^{-1} E_m / 2\pi$  is not very high.

Therefore, at high frequencies  $\omega \gg \omega_m$ , the compliance of the cell membrane prevails on its permeability and it follows that

$$F_m^{-1} = K_m + i\omega b E_m^{-1} \cong i\omega b E_m^{-1}, \quad (33)$$

and that

$$F_{cm}^{-1} = F_c^{-1} a i\omega b E_m^{-1} / (F_c^{-1} + a i\omega b E_m^{-1}) = F_c^{-1} / (1 + F_c^{-1} / a i\omega b E_m^{-1}) \quad (34)$$

If we assume  $F_c$  to have the typical form of equations (13, 15) as for gels

$$F_c = \eta_c = \eta_{0c} (\omega_{gc} / \omega)^\delta, \quad (\delta < 1/2) \quad (35)$$

it follows that

$$\begin{aligned} F_{cm}^{-1} &= \eta_c^{-1} (1 + \eta_c^{-1} / a i\omega b E_m^{-1}) = \eta_{0c}^{-1} (\omega_{gc} / \omega)^{-\delta} (1 + i (\omega_c / \omega_{gc}^\delta) \omega^{\delta-1}) \\ &= \eta_{0c}^{-1} ((\omega_{gc} / \omega)^\delta + i (\omega_c / \omega)) \end{aligned} \quad (36)$$

where

$$\omega_c = E_m / a b \eta_{0c} \quad (37)$$

$$\omega_{gc} = 2\pi \eta_{0c} / \rho_{fc},$$

and that the hydraulic admittance of the tissue reads

$$F_t^{-1} = \eta_g^{-1} [2(1-\gamma) \eta_g^{-1} + (1+2\gamma) \eta_c^{-1}] / \{(2+\gamma) \eta_g^{-1} + (1-\gamma) \eta_c^{-1} (1 + i (\omega_c / \omega_{gc}^\delta) \omega^{\delta-1})^{-1}\} \quad (38)$$

Since  $\delta < 1/2$ , at very high frequencies,  $\omega \gg (\omega_c / \omega_{gc}^\delta)^{1/(1-\delta)}$ , the imaginary part of  $F_{cm}$  tends to vanish, so that

$$F_{cm} \cong \eta_c \quad (39)$$

and hence

$$F_t^{-1} \cong \eta_g^{-1} \{ [2(1-\gamma) \eta_g^{-1} + (1+2\gamma) \eta_c^{-1}] / [(2+\gamma) \eta_g^{-1} + (1-\gamma) \eta_c^{-1}] \} \quad (40)$$

In figure 1 the admittance (40) of the tissue is shown as a function of  $\gamma$  for some values of the ratio  $\eta_g / \eta_c$ . Given that by (17) the US attenuation reads

$$\alpha_t / k = -1/2(c/c_{ft})^2 \omega(1 - \beta_{eg})(1 + \varepsilon\gamma) \rho_{11} \operatorname{Re}\{ F_t^{-1} \} \quad (41)$$

with the help of (40), the admittance of the tissue can be finally obtained.

In Figure 2 the normalized attenuation of the tissue  $\alpha_t(\gamma) / \alpha_t(\gamma=0) = (1 + \varepsilon\gamma) \operatorname{Re}\{ F_t^{-1} \}$  is depicted as a function of  $\gamma$  for some values of the parameter  $\varepsilon$ , where  $\varepsilon$  represents the normalized difference of the effective water content between the cells and the ECM that reads

$$\varepsilon = (\beta_{eg} - \beta_{ec}) / (1 - \beta_{eg}) \quad (42)$$

where it has been assumed  $\phi_g \cong \phi_c \cong \phi_t$ .

Introducing (40) into (41) after simple manipulation it follows that

$$(2\alpha/k) \cong -(c_t/c_0)^2 (\omega/\omega_g)^{1+\delta} (\omega_g/\omega_{gc})^\delta (1 - \beta_{eg})(1 + \varepsilon\gamma) \rho_{11} [2(1-\gamma)\eta_g^{-1} + (1+2\gamma)\eta_c^{-1} / (2+\gamma)\eta_g^{-1} + (1-\gamma)\eta_c^{-1}] \quad (43)$$

where from (25) it has been used the relation

$$1 - \beta_{et} \cong 1 - \beta_{eg} + \gamma \varepsilon (1 - \beta_{eg}) \cong (1 + \gamma \varepsilon) (1 - \beta_{eg}). \quad (44)$$

In the case when  $\eta_g^{-1} \ll \eta_c^{-1}$  it follows that the overall friction coefficient reads

$$F^{-1} \cong \eta_g^{-1} \{ (1+2\gamma) / (1-\gamma) \} \quad (45)$$

while for  $\eta_g^{-1} \gg \eta_c^{-1}$  it reads

$$F^{-1} \cong \eta_g^{-1} \{ (1-\gamma) / (1+\frac{1}{2}\gamma) \}. \quad (46)$$

When the cellular volume is a small part of the total volume of the tissue ( $\gamma \ll 1$ ) we obtain

$$F^{-1} \cong \eta_g^{-1} \{ 1-\gamma(2\eta_g^{-1} - 3\eta_c^{-1}) / (2\eta_g^{-1} + \eta_c^{-1}) \}, \quad (47)$$

that for  $\eta_c^{-1} \gg \eta_g^{-1}$  leads to

$$F^{-1} \cong \eta_g^{-1} (1+3\gamma), \quad (48)$$

while for  $\eta_g^{-1} \gg \eta_c^{-1}$  gives

$$F^{-1} \cong \eta_g^{-1} (1-\gamma). \quad (49)$$

By comparing formula (48) with (49) we can see that the angular coefficient of the  $\gamma$ -linear relation from positive (+3) for  $\eta_c^{-1} \gg \eta_g^{-1}$  changes to negative (-1) for  $\eta_g^{-1} \gg \eta_c^{-1}$ .

### 3. Experimental

#### 3.1. Materials and methods

Gel samples were prepared by dissolving 0.5 ml of an aqueous solution of sodium alginate at a concentration of 2% by weight (Alginic acid sodium salt from brown algae, Sigma A0682-1006) in

0,5 ml of  $\text{CaCl}_2$  solution (FLUKA 06991) at a concentration of 0.4% by weight to obtain the cross-linking of the polymer matrix.

The gel samples were refrigerated at  $-20\text{ }^\circ\text{C}$  for 24 h and then lyophilized at  $-40\text{ }^\circ\text{C}$  under vacuum for 12 hours.

The gel samples, in form of disks 0.3 cm thick and with a diameter of 1 cm, were inseminated by liver cells (of type HEPG2, Japanese isolated and immortalized hepatoblastic line (1997)) at various densities:  $0\text{ cells/cm}^3$ ,  $10^5\text{ cells/cm}^3$ ,  $2 \times 10^5\text{ cells/cm}^3$ ,  $5 \times 10^5\text{ cells/cm}^3$ ,  $10^6\text{ cells/cm}^3$ ,  $2 \times 10^6\text{ cells/cm}^3$ ,  $5 \times 10^6\text{ cells/cm}^3$ . The samples, one for each density value, were placed into an incubator at  $37\text{ }^\circ\text{C}$  for 30 minutes and then kept in a refrigerator at  $4\text{ }^\circ\text{C}$ . The experiments were carried out at room temperature of  $20 \pm 0,5\text{ }^\circ\text{C}$ .

The viability of the cells was checked at the end of the experiments. They were found alive at a percentage of about 85% with hexagonal-like parallelepiped shape. They were grouped in small compact clusters having a normal metabolism with low rate of replication.

The ultrasonic pulses were generated by the Panametrics® Pulser model 5052PR coupled with a PVDF piezoelectric transducer obtained in our laboratory following the Naganishi e Ohigashi procedure [21]. The US transducer is posed at the fixed wall of the cylindrical experimental cell. In front of the transducer there is a movable back-wall with a reflecting metal plate that is put in contact with the specimen during the US measurements. The transducer is used both as the source of the US wave as well as the receiver of US echoes.

The distance between the transducer and the reflecting iron layer behind the samples was measured with an accuracy of  $\pm 0.01\text{ cm}$ .

The US phase velocity is obtained by the measure of the time difference between two consecutive wave reflection.

The US absorption coefficient “ $\alpha$ ” was deduced by using the mathematical relation  $\alpha = \frac{1}{2d} \ln \frac{A_0}{A_{(2d)}}$ ,

where  $A_0$  and  $A_{(2d)}$  represent both the initial and final wave amplitude, respectively, and where  $d$  is the sample thickness.

The frequency of the ultrasonic wave generated by the Panametrics® Pulser model 5052PR used in the experimental tests were of 1 MHz .

By using electronic modules made in our laboratory, the US frequency of the pulser output was increased up to 1.4 MHz for a second set of measurements.

Echo Signal registration and conditioning data were collected with a routine and carried out with the LabView™ software on a computer through a National Instruments® DAQ device.

The water volume fraction of the hydrogel samples  $\beta = V_w / (V_w + V_p)$ , where  $V_w$  and  $V_p$  are the volume of water and polymer respectively, was obtained by means of the respective weight fractions  $P_w$  and  $P_p$  such as  $\beta \approx P_w / (P_w + P_p)$  since the water and Alginic acid (AA) specific densities are very close each other.

The fittings of the experimental results were carried out by means of a multiple parameter best fit utilizing the tool “custom equation” of the “curve fitting” section in MATLAB® 7.0 . Both the experimental US phase velocity and attenuation measurements where fitted by a parabolic custom equation.

### 3.2. Measurements of ultrasound velocity and attenuation

Before the US measurements on the porcine liver cells AA-scaffolds, the system was tested by measuring the US speed in distilled water at a temperature of 20°C. The results showed a precision of 0.2% with respect to the data in literature.

Figures 3 and 4 show the US phase velocity for the AA scaffolds with porcine liver cells at various concentrations together with the US velocity in the liver tissue (owing the value  $\gamma = 0.82$ ) at 1.4 MHz and at 1.0 MHz, respectively. The quadratic best-fits have been obtained for the values  $A1 = -1.4$ ,  $A2 = 1.7$  and  $A1 = -1.8$ ,  $A2 = 2.3$  at 1.4 MHz and at 1.0 MHz, respectively.

The US attenuation obtained for the AA scaffolds inseminated by porcine cells together with the attenuation of porcine liver are shown in Figure 5 and Figure 6. at 1.4 MHz and 1.0 MHz as a function of the cells volume fraction  $\gamma$ , respectively. The results show that exists a correlation between the conduct of the US velocity and attenuation. The similarity is due to the speed factor  $(c_t / c_{t0})^2$  in the US attenuation formula (41) .

Figure 7, for the US at 1.4 MHz, and figure 8, for the US at 1.0, MHz show the peculiar characteristics of the normalized attenuation  $\alpha_{t(\gamma)} / \alpha_{t(\gamma=0)}$  of the tissue.

The outcomes of the best fit procedure show that many couples  $(\eta_g / \eta_c, \varepsilon)$  of the poroelastic parameters are possible with practically the same minimum value of the root mean square distance. Therefore for the determination of the ratio  $\eta_g / \eta_c$ , we used the value of  $\varepsilon$  obtained by an independent way.

By introducing the measured values  $\beta_{eg} \cong 0.84$  for the AA gel scaffold and  $\beta_{ec} \cong 0.77$  for the cells, in the expression (25) we obtain the value  $\varepsilon \cong 0.43$  for the synthetic AAG-cells composite samples.

As far as it concerns for the liver ECM, given the measured value  $\beta_{eg} \cong 0.77$ , we obtain the value  $\varepsilon \cong 0$  for the liver tissue.

By using the experimental value  $\varepsilon \cong 0$ , the best-fits in Figure 7 and 8 give for the liver tissue (open triangles) the value  $\eta_g / \eta_c = 1.38$  and  $\eta_g / \eta_c = 1.32$  at 1.4 MHz and 1.0 MHz, respectively.

By introducing for the gel scaffold the value  $\varepsilon \cong 0.4$ , the best fit of figure 7 gives the value  $\eta_g / \eta_c = 2.24$  at 1.4 MHz.

Analogously, for the gel scaffold at 1.0 MHz the best fit of figure 8 gives the value  $\eta_g / \eta_c = 2.73$  ( $\varepsilon \cong 0.4$ ).

The results put in evidence that once the permeability of the extra-cellular gel scaffold  $\eta_g^{-1}$  is known or measured, the US poro-elastic model allows to derive the permeability of the cellular bulk  $\eta_c^{-1}$  and that one of the ECM.

In the present experiments, the permeability of the cells bulk  $\eta_c^{-1}$  results 1.32 times (at 1.0 MHz) and 1.38 times (at 1.4 MHz) bigger than that one of the ECM  $\eta_g^{-1}$  in liver. A more relevant difference exists between the cells bulk and the AA gel scaffolds permeabilities, where  $\eta_c^{-1}$  results 2.73 and 2.23 times bigger than  $\eta_g^{-1}$  at 1.0 MHz and at 1.4 MHz, respectively.

The reproducibility of the measures was sufficiently good with the variability of the experimental outputs leading to a R-square of the curve fitting of order of 90% .



#### 4. Discussion

The acoustic poroelastic model for soft living tissues describes the US propagation in terms of collective cells and ECM characteristics such as: (1) The permeability and the elasticity of the cells and of the ECM. (2) The percentage of cellular volume of the tissue. (3) The fractional volume of water of cells and of the ECM.

As far as it concerns the wave speed, the model, presented here, it does not make an theoretical derivation of the coefficients  $A_1$  and  $A_2$  as a function of the constituents of the cellular syncytium. Thence, the fits of the phase velocity data of Figure 3 and Figure 4 alone do not constitute any confirmation of the model. The important outcome is the fact that the parabolic behavior of the phase velocity appears also in the attenuation data (that are independently obtained) confirming the form of equation (41).

Moreover, subtracting the phase velocity contribution by the attenuation one, the normalized attenuation  $\alpha_{t(\gamma)} / \alpha_{t(\gamma=0)}$  of the cellular syncytium of the experiments (given in Figure 7 and in Figure 8) comes out with the appropriate shape shown by the theoretical one given in figure 1. It must be noted that the different values of the fitted  $\eta_g / \eta_c$  ratio (between Figure 7 and Figure 8) comes from the fact that the permeabilities,  $\eta_g$  and  $\eta_c$ , have a smooth dependence by the US frequency. The correspondence between the experimental points and the theoretical behavior gives us a preliminary evaluation of the experimental validity of the theory.

For sake of completeness, it must be noted that a better validation of the model would come from the direct measure of the poro-elastic constants of the cells and of the ECM by independent methods. On the other hand, this possibility encounters two major obstacles: 1) The extraction of the cellular content by the tissue alters the poroelastic characteristics of both the cells and the ECM, 2) The static

poroelastic values obtainable by the usual techniques may differ from the kinetic ones needed for US acoustic waves. Indeed, we tried to measure the elasticity and the permeability of the liver ECM alone but the cleavage of the cells resulted in changing very much its poroelastic characteristics.

The results show that on the base of the proposed model, it is possible to define an experimental method for the evaluation of the permeability of the cells and the ECM, once that one of the synthetic scaffold is known.

Moreover, by the contemporary measurement of US phase velocity and attenuation it is possible to evaluate the permeability ratio  $\eta_g / \eta_c$  between the liver cells and their ECM. Since the cirrhosis alters the elasticity and porosity of the ECM (and even of the liver cells) the model can potentially allow to detect and measure the advancement of the liver disease. This information compared with data from a set of liver tissues suffering the cirrhosis can allow the evaluation of the state of the illness in a generic patient.

Generally speaking, on the basis of epidemiological comparisons the technique can give information about the health state of biological soft tissues other than liver (as a sort of *eco-biopsy*) since, in addition to the elastic characteristics of the tissue, the longitudinal poroelastic waves depend also by the permeability of the cells and ECM.

As final remark, it must be noted that even if the model outputs agree with the results, the theory owns some subtle aspects that need to be considered carefully. Two of these regard the density of the bounded water, that cannot be directly measured, and its volume fraction. About the former point we can only retain that is approximately close to that of the free water (this is well sustainable since fluids are poorly compressible). As far as it concerns the latter one, the volume fraction of the bounded water has been measured in AA gel and is resulted to range between 2% and 12% [12], agreeing

with the hypothesis that is much smaller than that one the free water in hydrogels. Nevertheless, even being a small percentage, the bounded-water is not ineffective: the US phase velocity increase, due to the presence of 6% of bounded water, results to be of  $136 \text{ ms}^{-1}$  in AA gels [12] with respect to that of free water of  $1480 \text{ ms}^{-1}$ . In addition to that, since the bounded-water rheological properties sensibly differs from that of pure water (the variation of  $136 \text{ ms}^{-1}$  of the phase velocity, due to its presence, is quite relevant) we have also to expect that it will sensibly influence the temperature dependence of the sound velocity in tissues respect to that of pure water possibly furnishing an explanation of the remarkable variety of thermal behavior found in soft tissues.

Moreover, the polymer bounded water interaction has been considered here to be purely viscous without resonant states so that the outcomes of the theory takes into account just for the poroelastic structure-related US behavior. On the other hand, the water-protein resonances are widely present in living tissues. Currently, this is taken into account by modeling soft biological media as protein solutions [2]. Hence, the improvement of the present soft tissue model should necessarily come by the introduction of resonant frequencies into the bounded water-polymer interaction.

## **5. Conclusions**

The poroelastic continuum model for US propagation in hydrogels has been used to build up the acoustic wave equation for a tissue-like syncytium made of spherical cells homogeneously immersed in the ECM.

The model shows that the absorption of US is sensitive to the cellular content of the tissue as well as to the elasticity and permeability of cells and ECM.

When these parameters are influenced by the disease of a tissue, the model can possibly lead to the monitoring of the advancement of the illness by means of epidemiological comparisons.

The model preliminarily agrees with the experimental measurements done on porcine liver cells embedded in a poly-vinyl-alcohol matrix at various concentrations. The experimental results put in evidence that the porcine liver cells have the bulk permeability lower than that one of the AA gel (AAG) scaffold but about equal to that of its natural ECM.

## Nomenclature

$\varepsilon_{ij}$ = solid strain tensor	–
$e_{\alpha\alpha}$ = trace of the liquid strain tensor	–
$e^*_{\alpha\alpha}$ = trace of the bounded water strain tensor	–
$Q$ = gel poroelastic constant	$\text{N m}^{-2}$
$R$ = compressional gel poroelastic constant	$\text{N m}^{-2}$
$\beta$ = gel water volume fraction	–
$\phi$ = gel bounded water volume fraction	–
$\beta_e$ = gel effective free water volume fraction	–
$f$ = inverse of the hydraulic permeability of the gel	$\text{N s m}^{-4}$
$\rho_{11}$ = gel mass density parameter	$\text{Kg m}^{-3}$
$\rho_{12}$ = gel mass density parameter	$\text{Kg m}^{-3}$
$\rho_{22}$ = gel mass density parameter	$\text{Kg m}^{-3}$
$\rho_s$ = mass density of the gel solid network	$\text{Kg m}^{-3}$
$\rho_f$ = mass density of the gel interstitial liquid	$\text{Kg m}^{-3}$
$\rho$ = total gel mass density	$\text{Kg m}^{-3}$
$K$ = elastic constant of the polymer-bounded water interaction	$\text{N m}^{-2}$
$\eta$ = friction coefficient of the polymer-bounded water interaction	$\text{N s m}^{-4}$
$F$ = complex friction coefficient of the gel	$\text{N s m}^{-4}$
$c_0$ = pure elastic longitudinal US wave phase velocity of the gel	$\text{m s}^{-1}$
$c_f$ = phase velocity of the gel intermolecular fluid (free water)	$\text{m s}^{-1}$
$c_{f'}$ = phase velocity of the intermolecular fluid of the tissue	$\text{m s}^{-1}$
$c_{0t}$ = pure elastic longitudinal US wave phase velocity of the tissue	$\text{m s}^{-1}$
$c_t$ = longitudinal US wave phase velocity of the tissue	$\text{m s}^{-1}$
$\alpha$ = US attenuation coefficient	$\text{m}^{-1}$
$\eta_0$ = bounded water viscosity constant	$\text{N s m}^{-4}$
$\eta_{0c}$ = bounded water viscosity constant of the cell body	$\text{N s m}^{-4}$

$R_t$ = compressional poroelastic constant of tissue	$\text{N m}^{-2}$
$F_t$ = complex friction coefficient of the tissue	$\text{N s m}^{-4}$
$\beta_t$ = water volume fraction of the tissue	–
$R_g$ = compressional poroelastic constant of the ECM	$\text{N m}^{-2}$
$F_g$ = complex friction coefficient of the ECM	$\text{N s m}^{-4}$
$\beta_g$ = water volume fraction of the ECM	–
$R_c$ = compressional poroelastic constant of the cell body	$\text{N m}^{-2}$
$F_c$ = complex friction coefficient of the cell body	$\text{N s m}^{-4}$
$\beta_c$ = water volume fraction of the cell body	–
$\phi_g$ = bounded-water volume fraction of the ECM	–
$\phi_c$ = bounded-water volume fraction of the cell body	–
$\phi_t$ = bounded-water volume fraction of the tissue	–
$\gamma$ = cells volume fraction of the tissue	–
$F_m$ = complex friction coefficient of the cell membrane	$\text{N s m}^{-4}$
$K_m$ = hydraulic permeability of the cell membrane	$\text{N}^{-1}\text{s}^{-1} \text{m}^4$
$E_m$ = Young's elastic modulus of the cell membrane	$\text{N m}^{-2}$
$b^{-1}$ = cell membrane thickness	m
$a$ = cell diameter	m
$\varepsilon$ = normalized difference of the effective water content between the cells and the ECM	–

## References

- [1] M. L. Mather and C. Baldock, Ultrasound tomography imaging of radiation dose distributions in polymer gel dosimeters: Preliminary study, *Med. Phys.* 30, 2140–2148 (2003).
- [2] F. A. Duck, *Acoustic Properties of tissue at ultrasonic frequencies*, Academic Press, London, New York, 75-99 (1990), and references therein;
- F., W., Kremkau, R., W.; Barnes, C., P., McGraw, Ultrasonic attenuation and propagation speed in normal human brain, *J. Acoust. Soc. Am.* 70, 29-38 (1981); J., W., Wladimiroff, I., L., Craft, D., G., Talbert, In vitro measurements of sound velocity in human fetal brain tissue, *Ultrasound in Med. & Biol.* 1, 377-382 (1975).

- [3] X., Yang, R., O., Cleveland, Time domain simulation of nonlinear acoustic beams generated by rectangular piston with application to harmonic imaging , *J. Acoust. Soc. Am.*, 117-1, 113-123 (2005). J. C. Bacri, J. M. Courdille, J. Dumas, R. Rajaonarison, Ultrasonic waves: a tool for gelation process measurements , *J. Physiq. Lett.* 41, 369-372 (1980). A. Duck, *Acoustic Properties of Tissue at Ultrasonic Frequencies*, Academic Press, London, New York, 112-113 (1990).
- [4] M., A., Biot, General theory of three-dimensional consolidation , *J. Appl. Phys.* 12, 155-164 (1941).
- [5] M., A., Biot, Theory of propagation of elastic waves in a fluid-saturated porous solid , II high frequency range, *J. Acoust. Soc. Am.*, 28-2, 179-191 (1956).
- [6] M., A., Biot, Theory of propagation of elastic waves in a fluid-saturated porous solid, I low-frequency range , *J. Acoust. Soc. Am.*, 28-2, 168-178 (1956).
- [7] M., A., Biot, The elastic coefficients of the theory of consolidation , *J. Appl. Mech.* 24, 594-601 (1957).
- [8] D.L. Johnson, Elastodynamics of gels , *Journal of Chemical Physics* , 77, 1531-1539 (1982).
- [9] R.N. Chandler, Transient streaming potential measurements on fluid-saturated porous structures: an experimental verification of Biot's slow wave in the quasi-static limit , *Journal of Acoustical Society of America* 70, 116 (1981).
- [10] A. Peters, S.J. Candau, Kinetics of swelling of spherical and cylindrical gels , *Macromolecules* 21, 2278-2282 (1988).
- [11] D.L. Johnson, Equivalence between fourth sound in liquid He II at low temperature and the Biot slow wave in consolidated porous media , *Appl. Phys. Lett.* 37, 1065-1067 (1980).

- [12] P. Chiarelli et al, High frequency poroelastic waves in hydrogels , *J. Acoust. Soc. Am.* 127 , 3, 1197-1207 (2010).
- [13] Marianne Ziol et al, Noninvasive assessment of liver fibrosis by measurement of stiffness in patient with chronic hepatitis C , *Hepatology*, 41, 1, 48-54 (2005).
- [14] S. Lochhead, D. Bradwell, R. Chopra, and M. J. Bronskill, A gel phantom for the calibration of MR-guided ultrasound thermal therapy, *IEEE Ultrasonics Symposium*, Montreal, Canada (2004), Vol. 2, pp. 1481– 1483.
- [15] G. Divkovic, M. Liebler, K. Braun, T. Dreyer, P. Huber, and J. Jenne, Thermal properties and changes of acoustic parameters in an egg white phantom during heating and coagulation by high intensity focused ultrasound, *Ultrasound Med. Biol.* 33, 981–986 \_2007\_.
- [16] G. P. Berry, J. C. Bamber, C. G. Armstrong, N. R. Miller, and P. E. Barbonne, Toward an acoustic model-based poroelasticity imaging method: I. Theoretical foundation, *Ultrasound Med. Biol.* 32, 547–567 (2006).
- [17] J. Bercoff, M. Tanter, and M. Fink, Supersonic shear imaging: A new technique for soft tissue elasticity mapping, *IEEE Trans. Ultrason. Ferroelectr. Freq. Control* 51, 396–409.
- [18] Lochhead, S.; Bradwell, D.; Chopra, R.; Bronskill, M.J. A gel phantom for the calibration of MR-guided ultrasound thermal therapy , *Ultrasonics Symposium*, 2004 IEEE, 2, 23-27 Aug. 2004 Page(s): 1481-1483;
- G. Divkovic, M. Liebler, K. Braun, T. Dreyer, P. Huber, J. Jenne, Thermal Properties and Changes of Acoustic Parameters in an Egg White Phantom During Heating and Coagulation by High Intensity Focused Ultrasound , *Ultrasound in Medicine & Biology*, 33, 6981-986, (2007).
- (2004).

- [19] J. G. Berryman, Confirmation of Biot's theory, *Appl. Phys. Lett.* 37, 382–384 (1980).
- [20] Roth, B. J. The Electrical Conductivity of Tissues. *The Biomedical Engineering Handbook: Second Edition*. Ed. Joseph D. Bronzino, Boca Raton: CRC Press LLC, (2000).
- [21] Naganishi e Ohigashi, Ultrasonic transducers , United States Patent, October 20<sup>th</sup> (1981).

#### FIGURES CAPTIONS:

Figure 1: The theoretical behavior of the normalized soft tissue attenuation  $\alpha_{t(\gamma)} / \alpha_{t(\gamma=0)}$  as a function of the cell volume fraction  $\gamma$  for various values of the ratio  $\eta_g / \eta_c$  being  $\varepsilon = 0$ .

Figure 2: The theoretical behavior of the normalized soft tissue attenuation  $\alpha_{t(\gamma)} / \alpha_{t(\gamma=0)}$  as a function of the cell volume fraction  $\gamma$  calculated at various values of  $\varepsilon$  for the ratio  $\eta_g / \eta_c = 1,5$ .

Figure 3: Normalized phase velocity of the US fast wave in natural liver tissue (at  $\gamma = 0.82$ ) compared with the data obtained for the AAG-liver cells composite as a function of the cell volume fraction  $\gamma$  at a frequency of 1.4 MHz.



Figure 4: Normalized phase velocity of the US fast wave in natural liver tissue (at  $\gamma = 0.82$ ) compared with the data obtained for the AAG-liver cells composite as a function of the cell volume fraction  $\gamma$  at a frequency of 1.0 MHz.

Figure 5: Normalized attenuation of the US fast wave in natural liver tissue (at  $\gamma = 0.82$ ) compared with the data obtained for the AAG-liver cells composite as a function of the cell volume fraction  $\gamma$  at a frequency of 1.4 MHz.

Figure 6: Normalized attenuation of the US fast wave in natural liver tissue (at  $\gamma = 0.82$ ) compared with the data obtained for the AAG-liver cells composite as a function of the cell volume fraction  $\gamma$  at a frequency of 1.0 MHz.

Figure 7: Normalized natural liver tissue attenuation  $\alpha_{t(\gamma)} / \alpha_{t(\gamma=0)}$  (at  $\gamma = 0.82$ ) compared with the data obtained for the AAG-liver cells composite as a function of the cell volume fraction  $\gamma$  at a frequency of 1.4 MHz.

Figure 8: Normalized natural liver tissue attenuation  $\alpha_{t(\gamma)} / \alpha_{t(\gamma=0)}$  (at  $\gamma = 0.82$ ) compared with the data obtained for the AAG-liver cells composite as a function of the cell volume fraction  $\gamma$  at a frequency of 1.0 MHz.

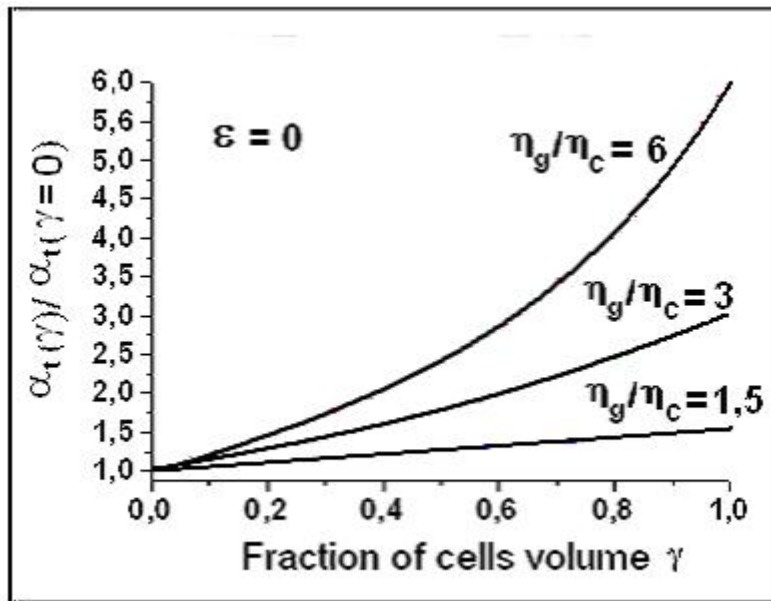


Figure 1

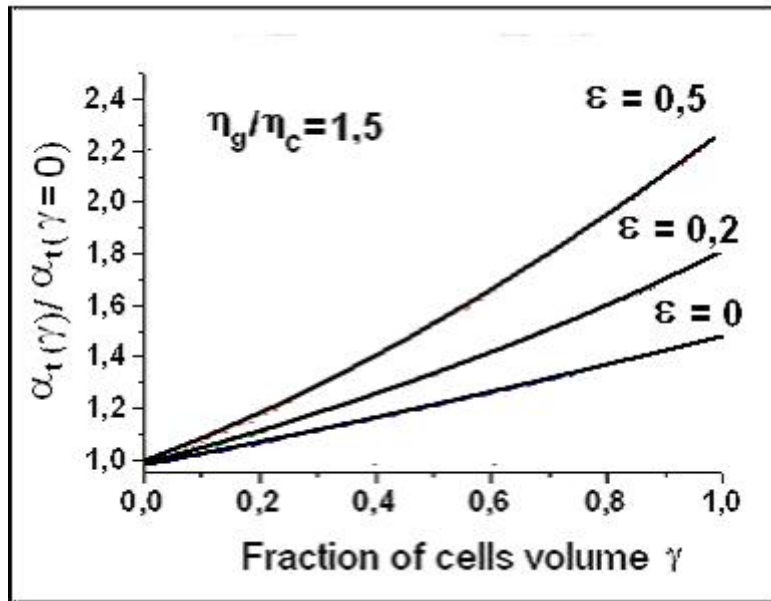


Figure 2

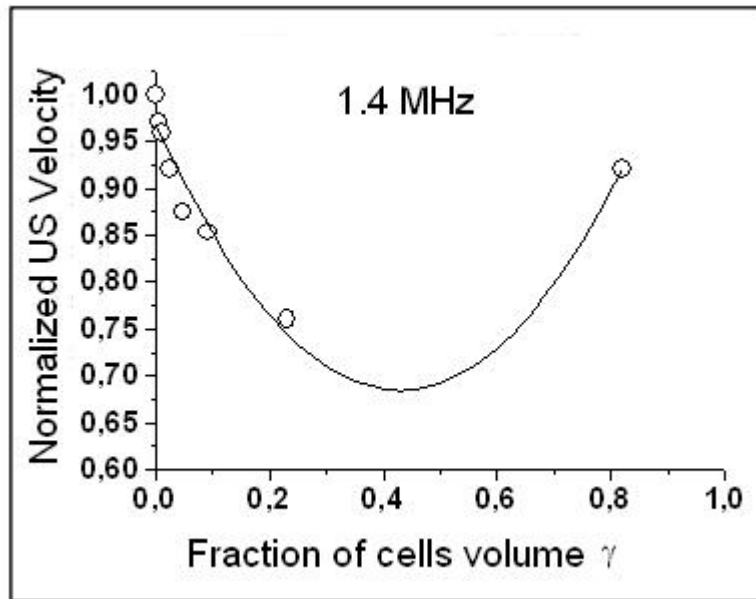


Figure 3

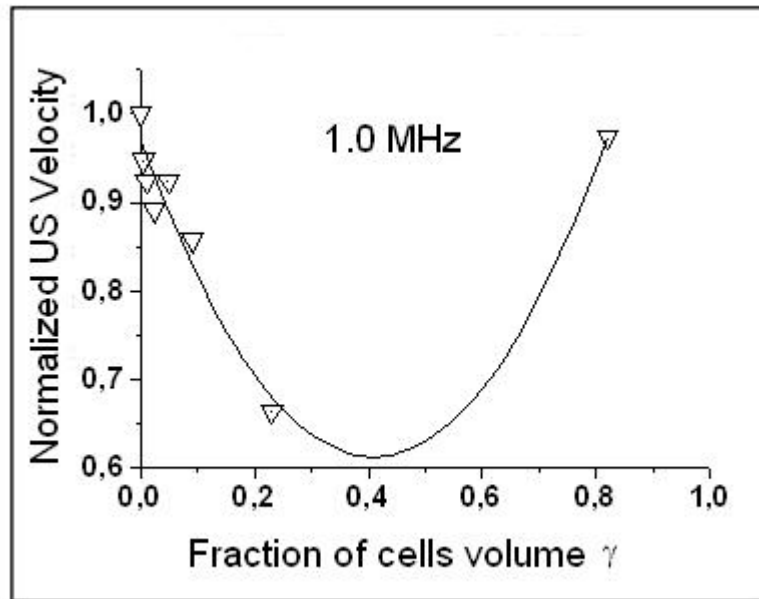


Figure 4

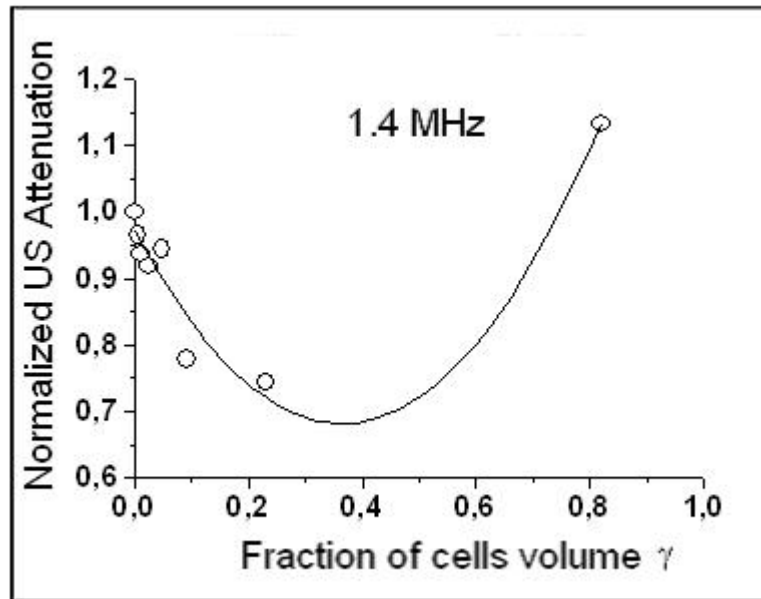


Figure 5

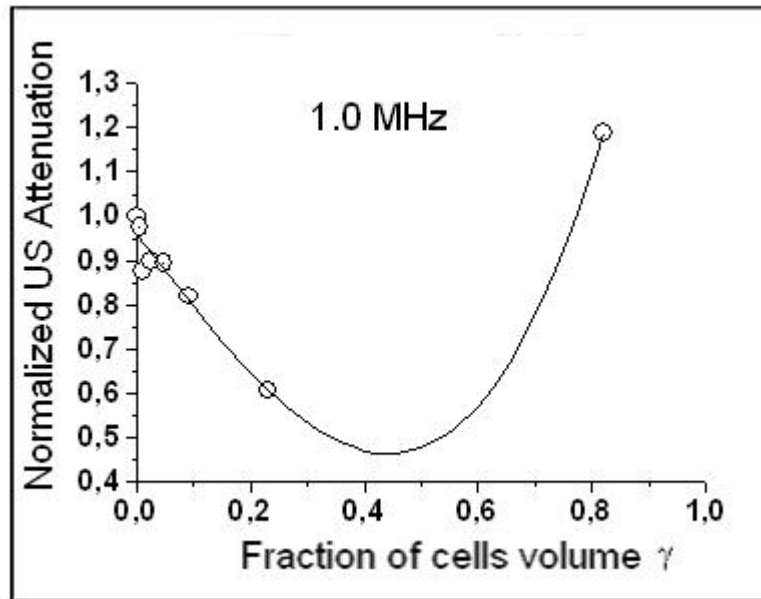


Figure 6

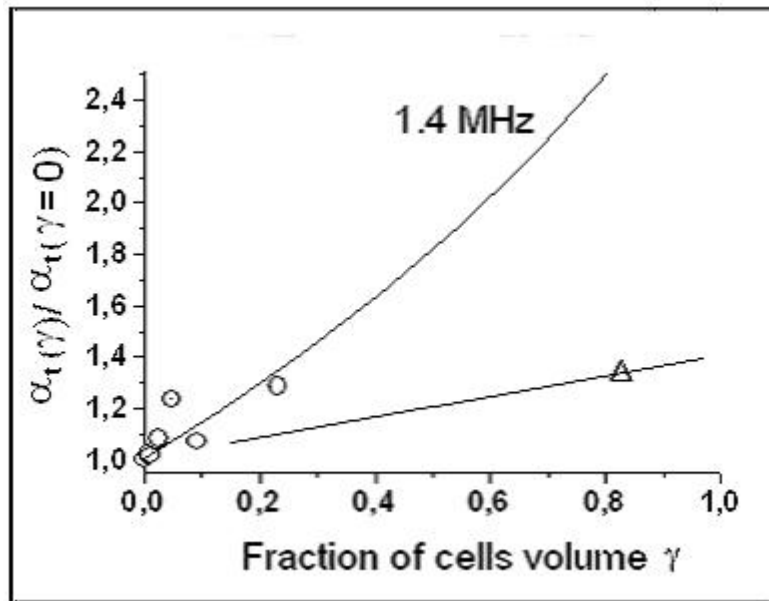


Figure 7



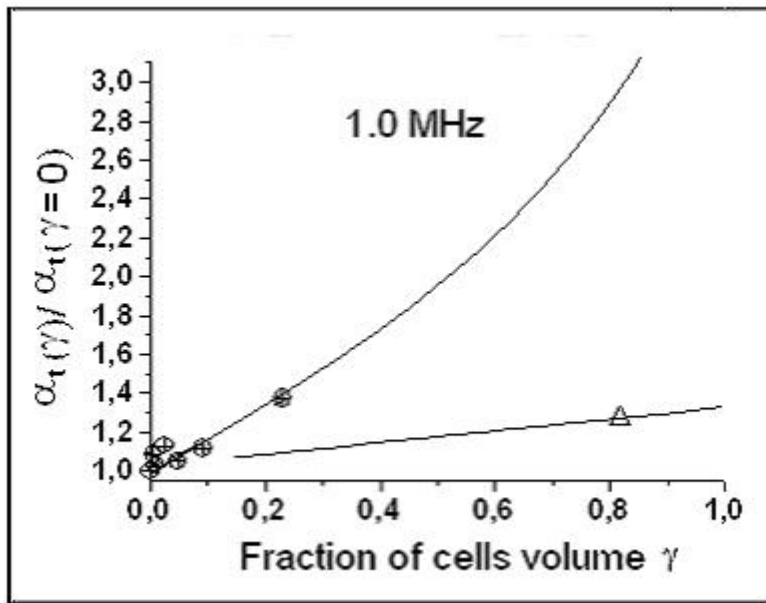


Figure 8